Decay Resistance of *Pterocarpus erinaceus* Poir. and the Antifungal Properties of its Extract

Lizhuan Zuo,[a,#] Mingxuan Qu,[a,#] Zhiru Song,[a] Yingying Zhang,[a] Xingyu Su,[a] Xianghua Yue,[a] Chuanfu Li,[b] and Bin Xu [a,*]

The processing residue of *Pterocarpus erinaceus* was used to obtain an ethanol-extract, whose anti-fungal properties and mode of action was investigated using multi-omics principles and gas chromatography-mass spectrometry. The results showed that the decay resistance of the heartwood of *Pterocarpus erinaceus* was in Grade I; it showed strong decay resistance. The effective concentration of 70% ethanol extract of the heartwood of *Pterocarpus erinaceus* was 13.8%. It showed high inhibition against *Coriolus versicolor* and *Gloeophyllum trabeum*, and the content of the extract was positively correlated with the diameter of the inhibition zone. Transcriptomics analysis showed there were 93 genes differentially expressed in *Gloeophyllum trabeum*. Among them, 42 genes were up-regulated and 51 genes were down-regulated. These genes were mainly related to oxidoreductase activity, integral components of the membrane, carbohydrate metabolism, lipid metabolism, and other related *Gloeophyllum trabeum* life activities. In total, 31 substances were separated and observed using GC-MS, and their peak areas accounted for 91.8% of the total peak area. Of these, 16 substances including ketones, esters, amines, alkanes, olefins and aromatic compounds showed a relatively high content. Ketones accounted for the most abundance at 29.1%. These compounds may represent the main active components of antifungal and decay resistance.

DOI: 10.15376/biores.18.2.4132-4142

Keywords: Pterocarpus erinaceus; Antifungal activity, Extract; Transcriptomics; GC-MS

*Contact information: a: College of Forest and Landscape, Anhui Agricultural University, Hefei, China, 230036; b: Chuanfu hongmu furniture Co., Ltd., Hefei, China; # The authors contributed equally to this work; *Corresponding author: xubin@ahau.edu.cn*

INTRODUCTION

Hongmu (*Pterocarpus erinaceus* of the Leguminosae family) is a popular hardwood species due to its unique color, good physical and mechanical properties, and natural durability (Shmulsky and Jones 2019). Presently, the manufacturing process of traditional Hongmu product is relatively complex, and the utilization rate of wood is less than 26% (Pan 2021). The residues generated in the manufacturing process have limited use, they have low added value, and they can pollute the environment. Therefore, there is an urgent need to find alternative uses for Hongmu processing residues. *Pterocarpus erinaceus* Poir. belongs to the *Pterocarpus* spp. according to the Hongmu standards (AQSIQ and SAC, 2017). *Pterocarpus erinaceus* is relatively abundant and therefore has a low price and a high market share (Senegal). As a result, its processing residues are abundant. *Pterocarpus erinaceus* has shown moderate activity against malaria, and its methanol extract has exhibited dose-dependent anti-inflammatory and analgesic effects

(Karou *et al*. 2003; Ouédraogo *et al*. 2016). Wood extract from the leaves, bark, and roots of *Pterocarpus erinaceus* have good inhibitory effects against common infectious bacteria (Tittikpina *et al*. 2018) including *Escherichia coli* (Griffin *et al.* 2016). The extract is a mixture of secondary metabolites that accumulate during the tree life and protect against environmental aggressors. Previous studies have shown that antifungal wood extracts lead to cell wall/membrane damage, altered gene/protein expression, and inhibition of enzyme activity, ranging from weak to strong for different wood extracts (Li 2012; Guan *et al.* 2021). It also shows local anti-inflammatory, antioxidant, lipoxygenase inhibition, and lipid peroxidation effects (Ouédraogo *et al.* 2017). In addition, it shows potential effects under clinical conditions requiring immune enhancement and anti-infection (Mahamat *et al.* 2018). Meanwhile, researchers have also studied the components and volatile components within the heart sapwood extract of *Pterocarpus erinaceus* (Liu *et al.* 2010; Tang *et al.* 2020).

Transcriptome refers to the collection of all RNA transcribed from a specific tissue or cell at a specific developmental stage or functional state. These proteins, working together, are capable of expressing the molecular mechanisms by which specific biological phenomena occur. Fueyo *et al.* (2012) reported that the mechanism of selective degradation of lignin by two saprophytic bacteria under the same condition. Martinez *et al.* (2009) studied the degradation mechanism of brown rot model beds by genome sequencing, secretome sequencing, and transcriptome sequencing. The development of the transcriptome in terms of bacteriostasis and antisepticity has been very rapid so far. Genes regulating lignin, cellulose, and hemicellulose degradation, and genome-wide differences in degradation processes are also reported (Floudas *et al.* 2015; Zhang *et al.* 2017). Therefore, studying the key genes and expression pathways that regulate cellulose at the RNA level can reveal the mechanisms of cellulose and lignin degradation by molecular biology. This approach has great significance in revealing the mechanism of wood extracts and its natural decay resistance. Although relevant studies on *Pterocarpus erinaceus* have been reported (Cai *et al*. 2019), there are still limited reports on the natural decay resistance of *Pterocarpus erinaceus* under laboratory conditions and its inhibition of wood rot fungi.

In this work, the decay resistance of *Pterocarpus erinaceus* was evaluated by a mass loss method. The extract of its processing residue was used as a raw material to produce 70% ethanol extraction. The inhibition performances of *Pterocarpus erinaceus* against *Coriolus versicolor* and *Gloeophyllum trabeum* were studied using a filter-paper method. Transcriptome sequencing technologies were combined to explore the molecular mechanism of its extract on the inhibition of *Gloeophyllum trabeum*. The main active components of its extract were analyzed *via* GC-MS. These results provide a basis for using the processing residues and using high-quality wood resources to increase their value.

EXPERIMENTAL

Materials

P. erinaceus processing residue was obtained from Anhui Chuanfu Hongmu Furniture Company (China). The processing residue (blocks) was ground into 40- to 60-mesh size material (diameter, 0.15 to 0.18 mm) after removing the oxidized surface, followed by further grinding to produce a powder, which was sealed and stored. The ethanol-extract (70% ethanol solution, Soxhlet extraction, 9 h) was filtered and processed by the heat reflow method (temperature, 90 °C), and the ethanol was recovered by rotary

evaporation in a water bath (da Silva *et al.* 2021). The extract was weighed and prepared as a water solution of 16 g/L, which was further diluted to 8 g/L, 4 g/L, 2 g/L, and 1 g/L by the double test tube diminishing dilution method. The extract was stored at -20 °C.

Coriolus versicolor and *Gloeophyllum trabeum* were chosen as candidates of white-rot fungus and brown-rot fungus, respectively. Both were provided by the China Center of Industrial Culture Collection (CICC).

Antimicrobial Assay

The decay resistance was evaluated based on GB/T 13942.1-2009. *C. versicolor* and *G. trabeum* were used. Heartwood from *P. erinaceus* was cut into 20 mm × 20 mm × 10 mm samples. The samples were dried in a blast drying oven at 40°C until the mass was constant. Culture bottles were filled with 200 mL of PDA medium (20% potato, 2% dextrose, and 2% agar), and the 3 samples were placed into each bottle. After 12 weeks, the samples were taken out, and hyphae and impurities on the surface were removed. The samples were oven-dried. The antimicrobial effect was evaluated based on the percentage of sample mass loss.

Antifungal Assay

The medium was prepared according to GB/T18261-2013. *C. versicolor* and *G. trabeum* were plate cultured. The antifungal performance was measured *via* filter paper, and the antifungal ability was determined by the size of the inhibition zone (Zhang 2009; Li 2014; Lakshmeesha *et al.* 2014). An inhibition zone with a diameter larger than 7 mm indicated positive antifungal activity. The control solutions were distilled water and 70% ethanol solution. Three replicates were conducted for each group.

Transcriptome Sequencing

PDA medium was inoculated with *C. versicolor and G. trabeum* by adding 2 mL of the diluted spore solution to a 200 mL Erlenmeyer flask and shaking at 220 rpm in an incubator set at 28 °C for 12 days. For the treatment group, 50 mg of *P. erinaceus* extract was added to the medium. After culturing for 48 h, the hyphae were collected for total RNA extraction. RNA was purified with oligo (dT) magnetic beads and fragmented by ultrasound. RNA was reverse transcribed to generate cDNA, treated with RNaseH to remove the RNA, and 5 mg of RNA was used for RNA-sequencing library preparation. The cDNA library was constructed and sequenced using the Illumina Hi-Seq 4000 platform and the 50-base single read sequencing method. Gene expression was normalized using the FPKM method with per million mapped reading per kilobase fragment (Mortazavi *et al*. 2008). An algorithm was used to identify differentially expressed genes at thresholds of a false discovery rate (FDR) $\leqslant$0.001 and an absolute value of log2 ratio $\geqslant$1 (Audic and Claverie 1997). Gene Ontology (GO) term enrichment analysis (Raw data were deposited at GEO, (https://www.ncbi.nlm.nih.gov/geo/, under accession number SRR18669264 and SRR18669265) and Kyoto Encyclopedia of Genes and Genomes (KEGG) pathway enrichment analysis were performed to understand the potential functions of the differentially expressed genes with two repetitions per group (The use of plant parts in the study complies with international, national and/or institutional guidelines.).

GC-MS Analysis

The analyses were performed on a GC-MS (Agilent 7890A, Santa Clara, USA) equipped with a 5975C mass spectrometer (Avondale, PA, USA). A HP-5MS capillary

fused silica column (30 m × 0.25 mm) was used for separation, and helium (99.999%) was used as carrier gas with a flow rate of 1 mL/min. The temperature program initiated at 60 °C (4 min), then 5 °C/min to 200 °C (5 min), and 4 °C/min to 280 °C (10 min). The injector temperature was 260 °C. A sample of 0.5 μL was injected in the split mode injection. The mass spectrometric data were recorded in the range of 50 to 500 m/z. The bombardment voltage was 70 eV and ionization source temperature was 230 °C.

RESULTS AND DISCUSSION

Analysis of Antimicrobial Properties

After 12 weeks under laboratory conditions, the natural durability of *P. erinaceus* was determined by measuring the mass loss rate samples following wood rot fungi exposure. Figure 1 shows the mass loss rates of the samples following infection with *C. versicolor* and *G. trabeum*.

It can be seen from Fig. 1 that the mass loss rate of *P. erinaceus* was 0.37% and 0.42% following inoculation with *C. versicolor* and *G. trabeum* fungi, respectively. According to the evaluation standard shown in Table 1, whilst inoculated with white rot fungus and brown rot fungus, the decay resistance grade of *P. erinaceus* was Grade I, reaching the degree of strong decay resistance.

Table 1. Standard of Natural Durability of Wood

Grade	Mass Loss Rate (%)	Decay Resistance
I	0-10	Strong
II	11-24	Good
III	25-44	Fair
IV	＞45	Bad

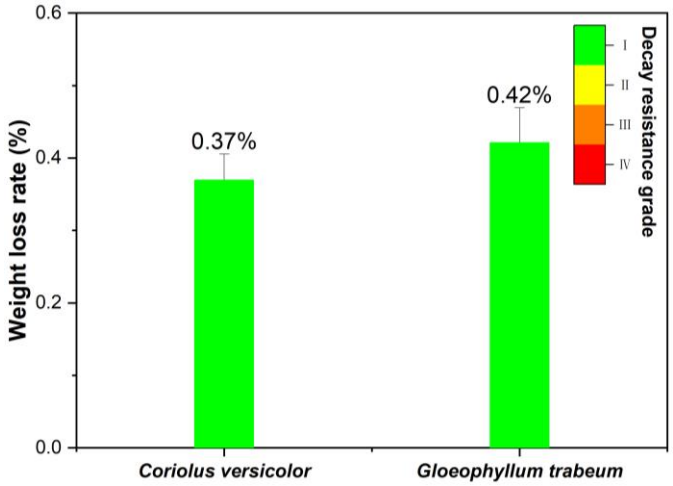

Fig. 1. Evaluation of the natural decay resistance grade of *P. erinaceus*

Analysis of Antifungal Properties

The 70% ethanol extract of *P. erinaceus* had distinct antifungal effects on the *C. versicolor* fungi (Fig. 2). Extracts of different concentrations had a positive correlation with the diameter of inhibition zone (Fig. 3a). Higher concentration of the extract showed increased antifungal effects. Moreover, the antifungal circle with the control group, where

only 70% ethanol was used, was very small (≤ 6 mm), and therefore the antifungal effect was ignored. Therefore, the effect of solvent on inhibition of *Coriolus versicolor* fungi could be excluded.

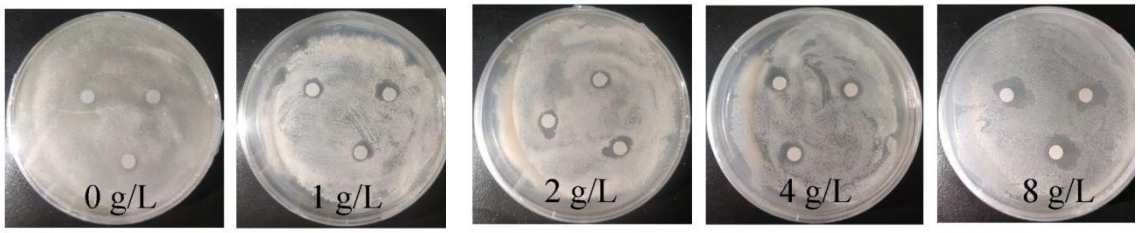

Fig. 2. Antifungal properties of 70% ethanol extract from *Pterocarpus erinaceus* on *Coriolus versicolor*

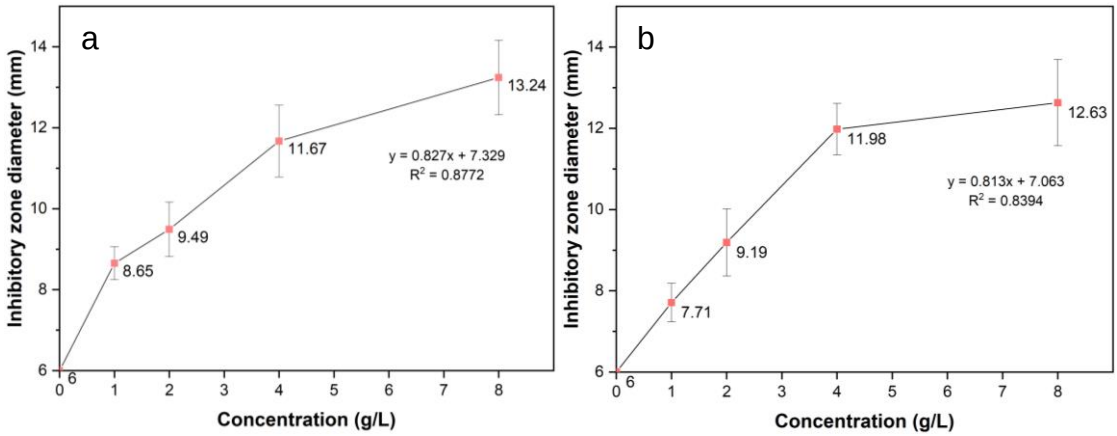

Fig. 3. Antifungal performance of concentrations of to *Coriolus versicolor* (a) and *Gloeophyllum trabeum* (b)

The 70% ethanol extract of *Pterocarpus erinaceus* had distinct antifungal effects on *Gloeophyllum trabeum* (Fig. 4). There was a positive correlation between extracts of different concentrations and the diameter of inhibition zone (Fig. 3b). The highest concentration of extract showed better antifungal effects. Moreover, the inhibition zone of the control group, where only 70% ethanol was administered, was very small (≤ 6 mm). Thus, the antifungal effect can be almost ignored, so the effect of solvent on *Gloeophyllum trabeum* fungi was excluded.

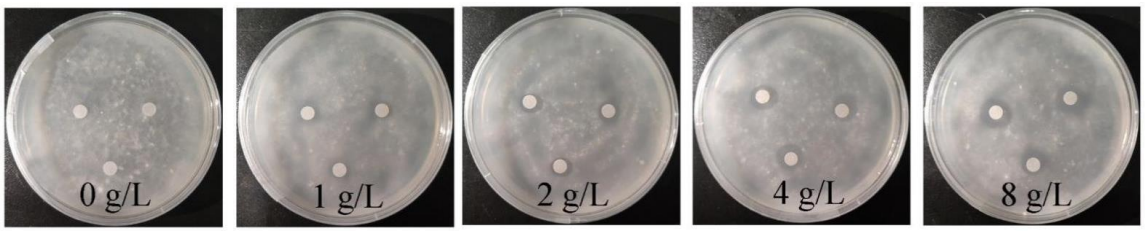

Fig. 4. The antifungal properties of 70% ethanol extract from *Pterocarpus erinaceus* on *Gloeophyllum trabeum*

Transcriptome Analysis

RNA-Seq sequencing results showed that a total of 10,209 genes were detected. Only 22 genes were expressed uniquely in the experimental group, and 11 genes were expressed only in the control group (Fig. 5a). Further, using the criteria of $p<0.05$ and $|\log_2 FC|>1$ to screen for differential genes, a total of 93 differentially expressed genes were obtained. Compared with the control group, the expression levels of 42 genes were up-regulated and the expression of 51 genes were down-regulated (Fig. 5b). At the same time, the differentially expressed genes were analyzed by hierarchical clustering. These results showed that compared with the control group, a large number of genes were differentially expressed in the experimental group (Fig. 5c).

To study the potential functions of the differentially expressed genes, GO enrichment analysis and KEGG enrichment analysis were performed (Fig. 6). The GO enrichment results showed that the differentially expressed genes were mainly enriched in related pathways such as oxidoreductase activity and membrane components. The KEGG enrichment results showed that differentially expressed genes were mainly enriched in related pathways such as carbohydrate metabolism and lipid metabolism. These results indicated that the extract may affect the oxidoreductase activity, integral component of membrane, carbohydrate metabolism, and lipid metabolism of *Gloeophyllum trabeum*, thereby inhibiting growth of the colony (Wang *et al.* 2020; Lv *et al.* 2022).

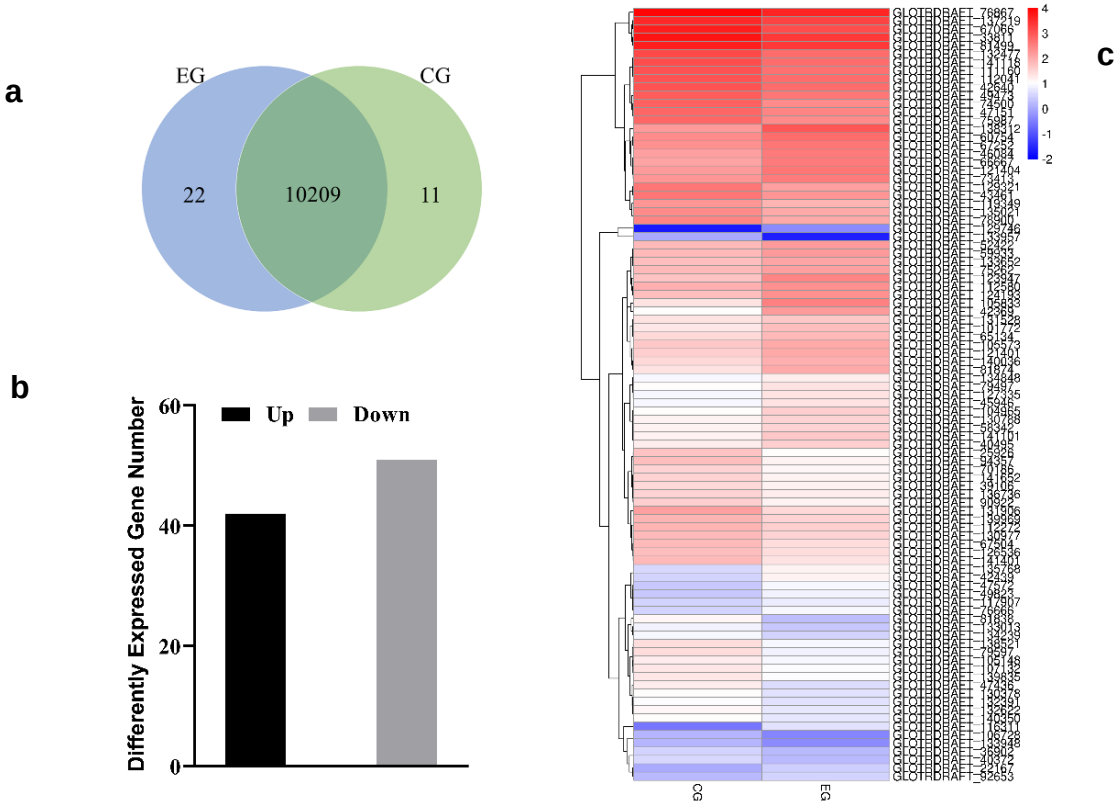

Fig. 5. Statistical analysis of differentially expressed genes. a) The number of shared genes and unique genes between the experimental and control groups; b) The number of up-regulated and down-regulated genes in the differentially expressed genes; c) Hierarchical clustering analysis of the differentially expressed genes between the experimental and the control group

Table 2. Content in 70% Ethanol Extract from *Pterocarpus erinaceus* Measured by GC-MS

No	Retention Time (min)	Relative Content (%)	Compound Name	Molecular Formula
1	7.62	1.95	1H-Trindene,2,3,4,5,6,7,8,9-octahydro-1,1,4,4,9,9-hexamethyl	$C_{21}H_{30}$
2	8.40	1.22	4-(4-Chlorophenyl)-2,6-diphenylpyridine	$C_{23}H_{16}ClN$
3	11.25	0.79	1,3,5,7,9-Pentaethylcyclopentasiloxane	$C_{10}H_{30}O_5Si_5$
4	12.02	0.12	Corydine	$C_{20}H_{23}NO_4$
5	14.86	0.35	3-Isopropoxy-1,1,1,5,5,5-hexamethyl-3-(trimethylsiloxy)trisiloxane	$C_{12}H_{34}O_4Si_4$
6	15.29	0.55	1-Adamantanecarboxamide, N,N-dimethyl	$C_{13}H_{21}NO$
7	17.86	0.17	Silane, trimethyl(4-phenylbutyl)	$C_{13}H_{22}Si$
8	20.74	1.00	Mercaptoacetic acid, bis(trimethylsilyl)	$C_8H_{20}O_2SSi_2$
9	20.89	2.72	Silane, [[5,5-dimethyl-4-methylene-2-(trimethylsilyl)-1-cyclopenten-1-yl]methoxy]trimethyl	$C_{15}H_{30}OSi_2$
10	22.75	0.81	Pentasiloxane, 1,1,3,3,5,5,7,7,9,9-decamethyl	$C_{10}H_{32}O_4Si_5$
11	24.57	1.65	Silane, 1,6-heptadiyne-1,7-diylbis[trimethyl-	$C_{13}H_{24}Si_2$
12	26.05	0.45	3-Oxa-6-thia-2,7-disilaoctane, 2,2,7,7-tetramethyl	$C_8H_{22}OSSi_2$
13	28.14	0.12	1,4-Benzenediol, 2,5-bis(1,1-dimethylethyl)	$C_{14}H_{22}O_2$
14	28.92	0.32	Silane, trimethyl[5-methyl-2-(1-methylethyl)phenoxy]	$C_{13}H_{22}OSi$
15	31.13	0.14	Pyrido[2,3-d]pyrimidine, 4-phenyl	$C_{13}H_9N_3$
16	31.74	0.43	1-Bromo-11-iodoundecane	$C_{11}H_{22}BrI$
17	31.93	0.33	Tetrasiloxane, decamethyl	$C_{10}H_{30}O_3Si_4$
18	32.36	0.16	Dodecahydropyrido[1,2-b]isoquinolin-6-one	$C_{13}H_{21}NO$
19	33.38	0.15	Formic acid, 1-(4,7-dihydro-2-methyl-7-oxopyrazolo[1,5-a]pyrimidin-5-yl)-, methyl ester	$C_{26}H_{26}F_2N_4O_3$
20	35.49	0.09	Cyclopentane, 1,1'-[3-(2-cyclopentylethyl)-1,5-pentanediyl]bis	$C_{22}H_{40}$
21	36.11	0.63	1,2-Benzisothiazole, 3-butoxy	$C_{11}H_{13}NOS$
22	37.24	0.05	Cyclotrisiloxane, hexamethyl	$C_6H_{18}O_3Si_3$
23	37.42	0.37	N-Methyl-1-adamantaneacetamide	$C_{13}H_{21}NO$
24	37.74	25.46	Dihydrojasmone	$C_{11}H_{18}O$
25	38.11	26.73	Pyridine-3-carboxylic acid, 6-carboxamide-N-(4-methylphenyl)-, methyl ester	$C_{15}H_{14}N_2O_3$
26	38.56	15.88	Ethanone, 2-hydroxy-1,2-bis(4-methoxyphenyl)	$C_{16}H_{16}O_4$
27	39.17	3.66	4-Hexanoylresorcinol	$C_{12}H_{16}O_3$
28	41.07	2.33	3,6-Dioxa-2,4,5,7-tetrasilaoctane, 2,2,4,4,5,5,7,7-octamethyl	$C_{10}H_{30}O_2Si_4$
29	43.45	2.21	Cyclopentanecarboxamide, 3-ethenyl-2-(3-pentenylidene)-N-phenyl-, [1.alpha.,2Z(E),3.alpha.]	$C_{19}H_{23}NO$
30	44.51	0.73	1,2-Bis(trimethylsilyl)benzene	$C_{12}H_{22}Si_2$
31	45.08	0.23	5-Benzofuranol, 2-ethoxy-2,3-dihydro-3,3-dimethyl-, methanesulfonate, (.+/-.)	$C_{13}H_{18}O_5S$

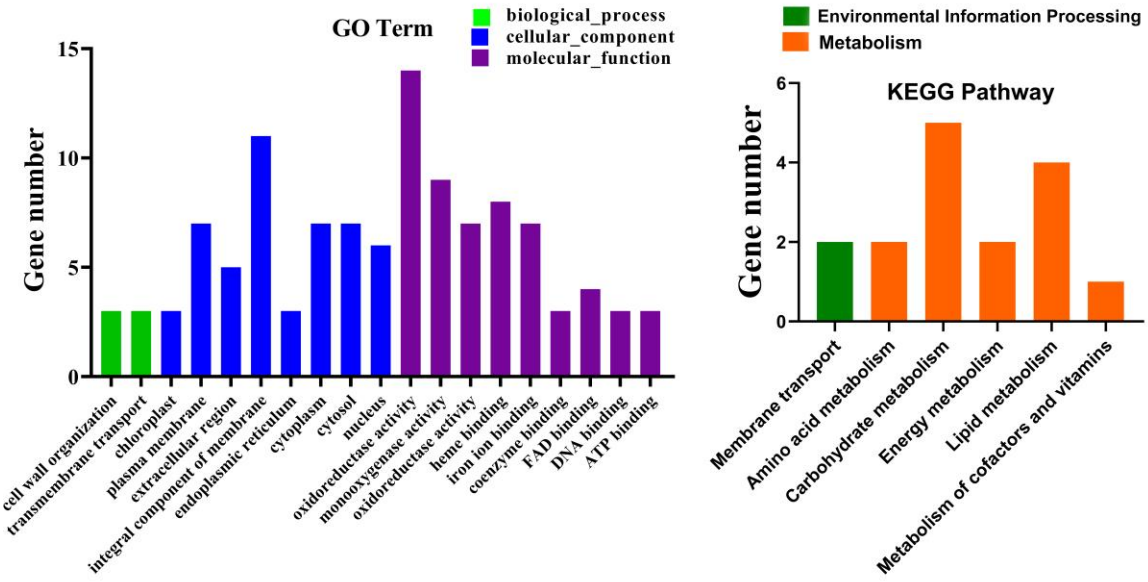

Fig. 6. GO and KEGG enrichment analysis of differentially expressed genes

GC-MS Analysis

GC-MS analysis of the 70% ethanol-extracted components revealed that 55 peaks were separated and 31 substances were tentatively identified in *P. erinaceus* (Table 2). These substances accounted for 91.8% of the total peak area, while 16 substances showed a relatively high abundance. The substances mainly included ketones, esters, amines, alkanes, olefins, and aromatic compounds. They contained 4 kinds of aromatic compounds, accounting for 18.46% of the total peak area. Alkanes and olefins were the second largest groups, accounting for 3.93% and 6.32% of the total peak area, respectively, where each contained 3 kinds of components. Ketones, esters, and amines accounted for 29.1%, 27.7%, and 2.76% of the total peak area, respectively. The most prominent compound was 3-pyridinecarboxylic acid. These compounds may represent the main active components responsible for the antifungal effect and decay resistance seen in *P. erinaceus* extracts (Zhou *et al.* 2015; Silva *et al.* 2017).

CONCLUSIONS

1. Under active attack by white rot fungus and brown rot fungus, the decay resistance of *P. erinaceus* was Grade I, reaching the degree of strong decay resistance.
2. There was high inhibition towards *C. versicolor* and *G. trabeum.* The concentrations of the extracts were positively correlated with the diameter of the inhibition zone. The extract might achieve inhibitory effects by affecting oxidoreductase activity, integral components of the membrane, carbohydrate metabolism and lipid metabolism, and related life activities in *G. trabeum*.
3. According to GC-MS analysis, 31 substances were tentatively identified in the extract, including ketones, esters, amines, alkanes, olefins, and aromatic compounds. Ketones accounted for most of the peak areas at 29.12%. These compounds may be the main active components of antifungal and decay resistance of *P. erinaceus*.

ACKNOWLEDGMENTS

This work was supported by the National Natural Science Foundation of China (31870538). Undergraduate Innovation and Entrepreneurship Training program of Anhui Agricultural University (S202110364186).

Declaration of Competing Interests

The authors declare that they have no known competing financial interests or personal relationships that could have appeared to influence the work reported in this paper.

Author Contributions

BX and LC conceived the materials and methodology. YX carried out the laboratory analyses. QM and SZ carried out the experiment and collected the data. ZY and SX contributed to the analysis and interpretation of data and wrote the main manuscript text. ZL helped in formal analysis, visualization, and writing.

Data Availability

All sequences access numbers are available in the NCBI database. The raw Illumina sequencing data were deposited in GenBank under Bioproject PRJNA824144 (https://www.ncbi.nlm.nih.gov/bioproject/PRJNA824144) with the accession numbers SRR18669264 and SRR18669265.

REFERENCES CITED

GB/T 13942.1-2009 (2009). "Natural durability of wood Part 1: Laboratory test methods for natural decay resistance," Standardization Administration of China, Beijing.

GB/T 18107-2017 (2017). "Hongmu," Standardization Administration of China, Beijing.

GB/T 1931-2009 (2009). "Wood moisture content determination," Standardization Administration of China, Beijing.

GB/T 35816-2018 (2018). "Method for analysis of forestry biomass raw materials: Determination of extract content," Standardization Administration of China, Beijing.

GB/T 18261-2013 (2013). "Method for efficacy of fungicides against wood mold and discoloration fungi," Standardization Administration of China, Beijing.

Audic, S., and Claverie, J. M. (1997). "The significance of digital gene expression profiles," *Genome Res.* 7, 986-995. DOI: 10.1101/gr.7.10.986

Cai, M. K., Lv, H. F., Cao, C., Zhang, L. P., Cao, R., and Xu, B. (2019). "Evaluation of antimicrobial activity of *Pterocarpus extracts*," *Ind. Crop. Prod*. 140, 13. DOI: 10.1016/j.indcrop.2019.111668

da Silva, R. S., do Nascimento Santos, D. K. D., and de Sousa, G. F. (2021). "Antifungical and immunomodulatory activities from *Caesalpinia pulcherrima* extracts," *Scientific Electronic Archives* 14. DOI: 10.36560/14920211454

Fernandez-Fueyo, E., Ruiz-Dueñas, F. J., and Ferreira, P. (2012). "Comparative genomics of *Ceriporiopsis subvermispora* and *Phanerochaete chrysosporium* provide insight into selective ligninolysis," *Proceedings of the National Academy of Sciences* 109, 5458-5463. DOI: 10.1073/pnas.1119912109

Floudas, D., Held, B. W., and Riley, R. (2015). "Evolution of novel wood decay mechanisms in Agaricales revealed by the genome sequences of *Fistulina hepatica*

and *Cylindrobasidium torrendii*," *Fungal Genetics and Biology* 76, 78-92. DOI: 10.1016/j.fgb.2015.02.002

Griffin, S., Tittikpina, N. K., Al-Marby, A., Alkhayer, R., Denezhkin, P., Witek, K., Gbogbo, K. A., Batawila, K., Duval, R. E., Nasim, M. J., Awadh-Ali, N. A., Kirsch, G., Chaimbault, P., Schafer, K. H., Keck, C. M., Handzlik, J., and Jacob, C. (2016). "Turning waste into value: Nanosized natural plant materials of *Solanum incanum* L. and *Pterocarpus erinaceus* poir with promising antimicrobial activities," *Pharmaceutics* 8, 12. DOI: 10.3390/pharmaceutics8020011

Guan, G. L., Zhang, L. N., Zhu, J. X., Wu, H., Li, W. X., and Sun, Q. J. (2021). "Antibacterial properties and mechanism of biopolymer-based films functionalized by CuO/ZnO nanoparticles against *Escherichia coli* and *Staphylococcus aureus*," *Journal of Hazardous Materials* 402, article 123542. DOI: 10.1016/j.jhazmat.2020.123542

Karou, D., Dicko, M. H., Sanon, S., Simpore, J., and Traore, A. S. (2003). "Antimalarial activity of *Sida acuta Burm*. f. (Malvaceae) and *Pterocarpus erinaceus* Poir. (Fabaceae)," *J. Ethnopharmacol*. 89, 291-294. DOI: 10.1016/j.jep.2003.09.010

Lakshmeesha, T. R., Sateesh, M. K., Prasad, B. D., Sharma, S. C., Kavyashree, D., Chandrasekhar, M., and Nagabhushana, H. (2014). "Reactivity of crystalline ZnO superstructures against fungi and bacterial pathogens: Synthesized using *Nerium oleander* leaf extract," *Cryst. Growth Des*. 14, 4068-4079.

Li, Q. (2014). *Research on Chemical Composition and Decay Resistance Mechanism of* Cinnamomum camphora *Wood Extracts*, Ph. D. Dissertation, Fujian Agriculture Forest University, FuZhou, China.

Li, X. (2012). *Study on the Antifungal Mechanism of Chinese Traditional Medicine Protection of Wood*, Ph. D. Dissertation, Mongolia Agriculture University, Huhehaote, China.

Liu, Z. Q., Zhang, R., Zhang, Z. H., Xiao, H. Y., and Liang, J. L. (2010). "Analysis on components of microwave-assist extracted volatile oil of *Pterocarpus erinaceus*," *Resource Development & Market* 26, 208-209.

Lv, H. F., Wang, Y. L., Qu, M. X., Zhang, Y. Y., Song, Z. R., Su, X. Y., and Xu, B. (2022). "Anti-fungal activity of *Dalbergia retusa* extract on *Gloeophyllum trabeum*," *Frontiers in Plant Science* 13. DOI: 10.3389/fpls.2022.906041

Mahamat, O., Christopher, T., Gilbert, A., Gerald, N. T., and Albert, K. (2018). "Immunological in vivo and in vitro investigations of aqueous extract of stem bark of *Pterocarpus erinaceus* Poir (Fabaceae)," *Am. J. Med. Sci*. 356, 56-63. DOI: 10.1016/j.amjms.2018.02.006

Martinez, D., Challacombe, J., Morgenstern, I., Hibbett, D., and Schmoll, M. (2009). "Genome, transcriptome, and secretome analysis of wood decay fungus *Postia placenta* supports unique mechanisms of lignocellulose conversion," *Proceedings of the National Academy of Sciences* 106, 1954-1959. DOI: 10.1073/pnas.0809575106

Mortazavi, A., Williams, B. A., McCue, K., Schaeffer, L., and Wold, B. (2008). "Mapping and quantifying mammalian transcriptomes by RNA-Seq.," *Nat. Methods* 5, 621-628.

Ouédraogo, N., Tibiri, A., Sawadogo, W. R., Yerbanga, S., Traore, M. C., Ouédraogo, S., Hay, A.-E., Garcia, I., and Guissou, I. P. (2016). "Anti-inflammatory and anti-plasmodial activities of methanol extract of *Pterocarpus erinaceus* poir. (Fabaceae) leaves," *Int. J. Pharmacol*. 12, 549-555. DOI: 10.3923/ijp.2016.549.555

Ouédraogo, N., Hay, A.-E., Ouédraogo, J. C. W., Sawadogo, W. R., Tibiri, A., Lompo, M., Nikiema, J.-B., N., Koudou, J., Dijoux-Franca, M.-G., and Guissou, I. P. (2017). "Biological and phytochemical investigations of extracts from *Pterocarpus erinaceus* Poir (Fabaceae) root barks," *Afr. J. Tradit. Complem*. 14, 187-195. DOI: 10.21010/ajtcam.v14i1.21

Pan, Z. H. (2021). "Survey and analysis of residual material utilization of redwood furniture enterprises," *Light Textile Industry and Technology* 50, 108-109. DOI: 10.3969/j.issn.2095-0101.2021.04.047

Shmulsky, R., and Jones, P. D. (2019). *Forest Products and Wood Science*, Wiley-Blackwell.

Silva, D. T., Herrera, R., Batista, B. F., Heinzmann, B. M., and Labidi, J. (2017). "Physicochemical characterization of leaf extracts from *Ocotea lancifolia* and its effect against wood-rot fungi," *International Biodeterioration* & *Biodegrad.* 117, 158-170. DOI: 10.1016/j.ibiod.2016.12.007

Tang, Y. J., Zhang, G. W., Xue, X. M., Xia, F., and Shi, H. F. (2020). "Component analysis of wood extract from precious tree species *Pterocarpus erinaceus* Poir," *Journal of Southwest Forestry University (Natural Science)* 40, 139-145. DOI: 10.11929/j.swfu.202002036

Tittikpina, N. K., Nana, F., Fontanay, S., Philippot S., Batawila, K., Akpagana, K., Kirsch, G., Chaimbault, P., Jacob, C., and Duval, R. E. (2018). "Antibacterial activity and cytotoxicity of *Pterocarpus erinaceus* poir extracts, fractions and isolated compounds," *J. Ethnopharmacol*. 212, 200-207. DOI: 10.1016/j.jep.2017.10.020

Wang, J, Chi, Z. Y., Zhao, K., Wang, H. F., Zhang, X., Xu, F., Shao, X. F., and Wei, Y. Y. (2020). "A transcriptome analysis of the antibacterial mechanism of flavonoids from *Sedum aizoon* L. against *Shewanella putrefaciens*," *World Journal of Microbiology and Biotechnology* 36(7), 1-14.

Xu, Y. M. (2019). *Wood Science*, China Forestry Publishing House, Beijing.

Zhang, L. (2009). *Study on the Antiseptic Effect of Ginkgo Tree Extract on Wood*, Nanjing Forest University Thesis.

Zhang, L., Wang, Z. X., Wang, Y., and Huang, B. (2017). "Transcriptomic profile of lignocellulose degradation from *Trametes versicolor* on poplar wood," *BioResources* 12, 2507-2527. DOI: 10.15376/biores.12.2.2507-2527

Zhou, N., Qi, J. Q., Wang, Y. G., Xie, J. L., Huang, X. Y., and Hu, Y. (2015). "GC-MS analysis of chemical components of essential oils from recent and ancient buried *Phoebe zhennan* woods," *Journal of Northwest A&F Uni: Natural Science Edition* 43, 136-140.

Article submitted: December 29, 2022; Peer review completed: April 1, 2023; Revised version received and accepted: April 13, 2023; Published: April 26, 2023.
DOI: 10.15376/biores.18.2.4132-4142